Redox Biology 78 (2024) 103434

Contents lists available at ScienceDirect

Redox Biology

journal homepage: www.elsevier.com/locate/redox

DKK3 as a diagnostic marker and potential therapeutic target for sarcopenia in chronic obstructive pulmonary disease

Zilin Wang [a,1], Mingming Deng [a,1], Weidong Xu [a], Chang Li [a], Ziwen Zheng [a], Jiaye Li [a], Liwei Liao [a], Qin Zhang [a], Yiding Bian [a], Ruixia Li [a,b], Jinrui Miao [a,b], Kai Wang [a], Yan Yin [c], Yanxia Li [d], Xiaoming Zhou [e], Gang Hou [a,*]

[a] National Center for Respiratory Medicine, State Key Laboratory of Respiratory Health and Multimorbidity, National Clinical Research Center for Respiratory Diseases, Institute of Respiratory Medicine, Chinese Academy of Medical Sciences, Department of Pulmonary and Critical Care Medicine, Center of Respiratory Medicine, China-Japan Friendship Hospital, Beijing, China
[b] Department of Pulmonary and Critical Care Medicine, The Second Affiliated Hospital of Harbin Medical University, Harbin Medical University, Harbin, China
[c] Department of Pulmonary and Critical Care Medicine, First Hospital of China Medical University, Shenyang, China
[d] Respiratory Department, The First Affiliated Hospital of Dalian Medical University, Dalian, China
[e] Department of Pulmonary and Critical Care Medicine, Disease, Fuwai Hospital, Peking Union Medical College, Chinese Academy of Medical Sciences, Beijing, China

ARTICLE INFO

Keywords:
Chronic obstructive pulmonary disease
DKK3
Sarcopenia
Mitochondrial dysfunction
CKAP4

ABSTRACT

Sarcopenia, characterized by the progressive loss of muscle mass and function, significantly affects patients with chronic obstructive pulmonary disease (COPD) and worsens their morbidity and mortality. The pathogenesis of muscle atrophy in patients with COPD involves complex mechanisms, including protein imbalance and mitochondrial dysfunction, which have been identified in the muscle tissues of patients with COPD. DKK3 (Dickkopf-3) is a secreted glycoprotein involved in the process of myogenesis. However, the role of DKK3 in the regulation of muscle mass is largely unknown. This study investigated the role of DKK3 in COPD-related sarcopenia. DKK3 was found to be overexpressed in cigarette smoking-induced muscle atrophy and in patients with COPD. Importantly, plasma DKK3 levels in COPD patients with sarcopenia were significantly higher than those without sarcopenia, and plasma DKK3 levels could effectively predict sarcopenia in patients with COPD based on two independent cohorts. Mechanistically, DKK3 is secreted by skeletal muscle cells that acts in autocrine and paracrine manners and interacts with the cell surface-activated receptor cytoskeleton-associated protein 4 (CKAP4) to induce mitochondrial dysfunction and myotube atrophy. The inhibition of DKK3 by genetic ablation prevented cigarette smoking-induced skeletal muscle dysfunction. These results suggest that DKK3 is a potential target for the diagnosis and treatment of sarcopenia in patients with COPD.

1. Introduction

Chronic obstructive pulmonary disease (COPD) is characterized by consistent respiratory symptoms and restricted airflow [1] with frequent comorbidities affecting the cardiovascular, gastrointestinal, hematological, and musculoskeletal systems [2]. Patients with COPD have diminished exercise performance due to impaired skeletal muscle function, which is linked to poor prognosis, higher hospitalization rates, and increased morbidity and mortality. Previous studies have indicated that 15.5–34 % of patients with stable COPD also have sarcopenia [3], which is defined as a progressive loss of muscle mass and strength [4]. Individuals with stable COPD who also exhibit sarcopenia have diminished exercise capacity and elevated dyspnea index scores. Concurrently, this decline in physical activity leads to disuse atrophy, further exacerbating the cycle of disease progression [5].

Skeletal muscle is a dynamically stable tissue, and the maintenance of its normal function relies on a balance between protein synthesis and degradation that is controlled by several factors [6]. In patients with COPD, several factors contribute to reduced protein synthesis and increased protein degradation [7], including cigarette smoke, inflammatory mediators, and oxidative stress components. Collectively, these factors lead to a negative protein balance, decreasing the quality and

* Corresponding author.
E-mail address: hougangcmu@163.com (G. Hou).
[1] These authors share the first authorship.

https://doi.org/10.1016/j.redox.2024.103434
Received 6 September 2024; Received in revised form 11 October 2024; Accepted 16 November 2024
Available online 17 November 2024

functionality of skeletal muscle tissues, and ultimately resulting in muscle atrophy [8,9]. In addition, various mitochondrial quality control defects, including mitochondrial respiratory chain dysfunction [10,11] and enhanced mitophagy signaling [12,13], have been identified in the muscle tissues of patients with COPD. These defects lead to decreased skeletal muscle oxidative capacity and fatigue resistance, leading to muscle atrophy [14,15]. Overall, the development and progression of muscle atrophy in patients with COPD are regulated by complex and varied mechanisms.

Dickkopf-related protein 3 (DKK3), a secreted glycoprotein, belongs to the Dickkopf (DKK) family (DKK1, DKK2, DKK3 and DKK4) [16]. Unlike other DKK family members which can bind the Wnt co-receptor Lrp5/6 and Kremen proteins to inhibit Wnt signaling [17,18], DKK3 does not bind these receptors [19,20]. However, The exact receptor for DKK3 has not yet been determined. DKK3 may play a role in myogenesis. In zebrafish, it enhances phosphorylated p38α levels, initiating Myf5 transcription via Integrin α6b [21,22]. This process is regulated by a feedback loop involving miR-3906, which is encoded by the first intron of Myf5 and inhibits DKK3 translation, controlling embryonic myogenesis [23]. In contrast, a recent study [24] reported that DKK3 suppresses impedes muscle regeneration via impeding muscle stem cell differentiation in mice. DKK3 knockdown may rescue muscle regeneration defects in Baf60c muscle-specific knockout obese mice. Despite these findings, the functions of DKK3 in muscle mass regulation remains ambiguous.

This study investigated the role of DKK3 in COPD-related sarcopenia. The clinical value of DKK3 in patients with COPD was assessed and the underlying mechanisms by which DKK3 contributes to mitochondrial dysfunction and muscle atrophy were explored. In addition, the therapeutic potential of blocking DKK3 signaling to counteract smoking-induced muscle wasting was investigated.

2. Materials and methods

2.1. Human samples analyses and data measurements

Plasma samples from 23 age-matched healthy controls were collected at the China Medical University. Human plasma samples were collected from patients with stable COPD at the First Hospital of Dalian Medical University (n = 117 as the training set) and First Hospital of China Medical University (n = 118 as the validation set) between August 2018 and December 2019 (approval number: 2018-144-2). The plasma DKK3 concentration was quantified using a commercial enzyme-linked immunosorbent assay (ELISA) kit (DY1118, R&D Systems, USA).

Stable COPD was diagnosed based on the Global Initiative for Chronic Obstructive Lung Disease (GOLD) guidelines, and sarcopenia was diagnosed according to the Asian Working Group for Sarcopenia (AWGS) 2019 criteria: low muscle mass [bioelectrical impedance (males, <7.0 kg/m^2; females, <5.7 kg/m^2)], low muscle strength [handgrip strength (HGS) (males, <28 kg; females, <18 kg)], and/or poor physical performance [5-time chair stand test (5STS), ≥12 s]. The functional assessments conducted in this study have been described previously [25–27]. In brief, the muscle mass was measured by BIA (InBody770; InBody, Seoul, South Korea). The 6-min walking distance (6MWD) was assessed according to the American Thoracic Society guidelines. in a 30-m, flat, straight, enclosed corridor. The corridor was marked at 3-m intervals, with cones indicating turnaround points and a brightly colored tape denoting the starting line. The participants were instructed to walk as far as possible in 6 min along the 30-m, flat, straight, enclosed corridor, with allowances for rest if needed, and laps tracked by a counter. During the five-time sit-to-stand test, the participant was seated on a 48 cm high, armless chair with hands folded across the chest, performing the sit-to-stand action five times as quickly as possible, with the time taken recorded. This test was repeated three times with 1-min rest intervals, and the average time was recorded. The thickness and cross-sectional area of quadriceps rectus femoris were measured using Gray-scale ultrasound with 4-to15-MHz linear-array transducer (SuperSonic Imagine, Aix-en-Provence, France) and performed by two trained physicians. The patient avoided strenuous exercise for 72 h, rested for 15 min, and then lay supine on the operating table with relaxed muscles. An ultrasound probe was positioned perpendicular to the dominant leg to measure RFthick and RFcsa by outlining the rectus femoris inner echogenic line on a static image. The average of three consecutive measurements within 10 % variance was recorded. All participants provided written informed consent.

2.2. Animal model

The animal experiments were approved by the Animal Ethics Committee of the China-Japan Friendship Hospital. Six-to eight-week-old male C57BL/6J mice were purchased from Beijing HFK BIOSCIENCE Co., Ltd. (Beijing, China). Mice were exposed to CS using a systemic exposure system (KT-YQSB-0634, Research Institute of Tsinghua University in Shenzhen, Shenzhen, China) within a barrier facility. The cigarette smoke was delivered to the exposure chamber in a controlled and consistent manner to ensure steady delivery and concentration throughout the exposure period described previously [28,29]. Each exposure session involved the combustion of 20 cigarettes (Carbon monoxide 10 mg, Tar 10 mg, Nicotine 0.8 mg). Smoke was delivered to the mice twice daily for six days a week for a three-month period. The cigarette smoke was delivered to the exposure chamber in a controlled and consistent manner to ensure steady delivery and concentration throughout the exposure period. Control mice were exposed to fresh air. The mice were housed under standard conditions with a 12-h light/dark cycle and given ad libitum access to food and water.

2.3. Grip strength test

To measure the grip strength of the mice, we used a grip strength meter (YLS-13A, China) for both forelimbs and hind limbs. Before each measurement, the meter was calibrated to zero. During the test, the mouse's tail was gently pulled back at a consistent speed while it grasped a grid. The peak force was recorded when the mouse released the grid. Five measurements were taken at 3-s intervals. All tests were conducted by a single operator to ensure consistency and reliability.

2.4. Muscle virus injection

Adeno-associated virus serotype 9 (AAV9) vectors encoding shRNA against DKK3 (AAV9-shDKK3) or non-targeting scrambled shRNA (AAV9-shCtrl) were intramuscularly injected into the TA muscles of the C57BL/6J mice two weeks prior to CS and again eight weeks after its initiation. Each injection included 50 μl of viral solution at a concentration of 1×10^{12} viral genomes/ml. The AAV9 vectors were custom-engineered and supplied by Hanbio Tech (Shanghai, China). The TA muscles were harvested four weeks after the final injection. Each treatment group consisted of five mice. The sequences for AAV-shDKK3 were as follows:

sense, GGAGCCAUGAAUGUAUCAUT

antisense, AUGAUACAUUCAUGGCUCCTT.

2.5. C2C12 cell culture, differentiation and lentivirus transduction

C2C12 myoblasts obtained from the China Infrastructure of Cell Line Resource were cultured in DMEM supplemented with 10 % fetal bovine serum. At 70–80 % confluence, cell differentiation was initiated by transferring the cells to DMEM containing 2 % horse serum (differentiation medium) for six to seven days, during which the medium was renewed every other day. In addition, stable cell lines were established via lentiviral transduction expressing either scrambled shRNA or shRNAs targeting DKK3, followed by puromycin selection and differentiation. For DKK3 knockdown C2C12 stable cell line, we stably

transduced C2C12 cells with lentivirus expressing non-sense shRNA (shNC) or DKK3 targeting shRNA (shDKK3) prior to CSE treatment.

2.6. Conditioned medium preparation and recombiant human DKK3 treatment

C2C12 cells were seeded in culture dishes and allowed to differentiate. Then the myotubes were transfected with pcDNA3.1 plasmids encoding DKK3 protein (OEDkk3) or empty pcDNA3.1 (pcDNA) as control. Six hours after transfection, the differentiation medium was replaced with DMEM medium with 0.1 % bovine serum albumin (BSA). After two days, the supernatant was harvested, centrifuged to remove cell pellet (1200 rpm 5 min), filtered using a 0.2-μm filter, and stored at −80 °C for future use. For the CM treatment, C2C12 myoblasts were differentiated for four days, then the culture medium was replaced with CM, a mixture of differentiation medium and supernatant in a 1:1 ratio, for two days. Then, the myofiber size was evaluated. For the DKK3 treatment, C2C12 myotubes that differentiated for four days were treated with recombinant human DKK3 (rhDKK3, 150 ng/mL) (HY–P7812, MCE, China) for 48 h after transiently transfected with siRNA.

2.7. Mitochondrial membrane potential

To evaluate the mitochondrial membrane potential, the C2C12 cells were stained with JC-1 dye from the JC-1 MitoMP detection kit (Dojindo, Kumamoto, Japan) according to the manufacturer's guidelines. The staining protocol involved incubating the cells with 1 μg/mL JC-1 at 37 °C for 20 min followed by three washes with HBSS. Fluorescence signals were captured from at least five fields for each of the four biological replicates per group, using a Nikon fluorescence microscope. The images were analyzed using ImageJ software.

2.8. Cellular respiration assay

The oxygen consumption rate (OCR) of C2C12 cells was measured using a Seahorse XF Pro Analyzer according to the manufacturer's instructions. C2C12 cells, divided into following groups (Ctrl, OE-DKK3, shNC, and shDKK3), were seeded in 96-well plates. The shNC and shDKK3 groups were treated with 2 % CSE 48 h before the assay. OCR was measured under basal conditions and following sequential additions of oligomycin (20 μL), FCCP (22 μL), and rotenone + antimycin A (25 μL). Respiration rates were automatically calculated by Seahorse XFe Assay Version (2.6.3.5).

2.9. Myofiber diameter and cross-sectional area

The myofiber diameter and cross-sectional area were measured using ImageJ software. At least five visual fields were randomly selected for each of the biological replicates. All fibers from each visual field were measured. The measurements were performed in a blinded manner to ensure unbiased results.

2.10. Statistics

All statistical analyses were conducted using GraphPad Prism software (version 10). Intergroup differences between two groups were assessed using a two-tailed unpaired Student's t-test and one-way analysis of variance and multiple subsequent comparisons using Tukey-Kramer corrections (normally distributed data) and the Kruskal-Wallis test complemented by Dunn's multiple comparison test (non-normal distribution) were used to compare differences between more than two groups. In human sample studies, the correlation between plasma DKK3 concentrations and clinical variables was analyzed using Pearson's correlation. Receiver operating characteristic curve (ROC) analysis was used to predict clinical efficacy.

3. Results

3.1. DKK3 is overexpressed in cigarette smoking-induced muscle atrophy and patients with COPD and sarcopenia

To investigate the underlying mechanism in cigarette-smoking induced muscle atrophy, we constructed the cigarette-smoking (CS) mice model. After 12 weeks of exposure to smoke (Fig. 1a), mice in the CS group were histologically confirmed to have emphysema, with a significantly decreased mean linear intercept (MLN) and an increased mean alveolar number (MAN) (Fig. 1b and c). The body weight changes over 12 weeks in mice exposed to air or CS were recorded. The CS mice exhibited significantly lower body weights from week 8 onwards (Supplemental Fig. 1). Mice in the smoke exposure group had reduced grip strength (Fig. 1d) and significantly lower ratios of Quad (quadriceps), Gast (gastrocnemius) and TA (tibialis anterior) muscle weight to body weight than those of mice in the control group (Fig. 1e and f). Myofiber size evaluated in cross-sectional area (CSA) was reduced in the CS mice (Fig. 1g and h). To explore differently expressed genes in CS-related muscle atrophy, RNA sequencing was conducted and revealed that 44 % (832) of the genes were significantly upregulated and 56 % (1050) were downregulated in the muscles of the CS mice. The Kyoto Encyclopedia of Genes and Genomes and Gene Ontology analysis revealed enhanced activated protein digestion, absorption, and cellular processes in the muscles of CS mice (Fig. 1i). DKK3, a divergent member of dickkopf family, emerged as a significant focus of our study and was increased by more than four-fold in the muscles of the CS mice. Consequently, we preliminarily validated the expression levels of DKK3 in both the CS mouse model and CSE-treated C2C12 myotubes. The upregulation of DKK3 protein was confirmed via immunoblotting of the CS muscle tissue (Fig. 1j and k). A previous study reported that myofibers were the major source of DKK3(30). We further investigated the expression of DKK3 protein in CSE-treated C2C12 myotubes and the corresponding myotube atrophy. The protein level of DKK3 was upregulated and MyHC was downregulated in C2C12 cells, as determined using western blotting (Fig. 1l and m). Given that DKK3 is a secretory protein [16], we examined its expression levels in the plasma of CS mice model and patients with COPD. The plasma DKK3 levels in mice were detected and DKK3 upregulation in circulation was also confirmed by ELISA (Fig. 1n). Similar to that in CS mouse models, the plasma DKK3 protein levels were increased in patients with stable COPD (n = 53) compared to those in age-matched healthy controls (n = 23) (Fig. 1o). Taken together, these results confirmed that DKK3 was elevated in patients with COPD, smoke-exposed mice, and CSE-treated C2C12 myotubes. Furthermore, we sought to explore the relationship between DKK3 and skeletal muscle function, mass, and exercise capacity.

3.2. Elevated Plasma DKK3 Levels Correlate with Disease Severity and Muscle atrophy in patients with COPD

We next investigated the correlation of plasma DKK3 level with skeletal muscle in COPD patients, assessing both quality and quantity. Patients with COPD and sarcopenia had higher plasma DKK3 levels than patients with COPD without sarcopenia (Fig. 2a). Next,we evaluated the correlation between plasma DKK3 level and exercise tolerance in patients with COPD. The plasma DKK3 concentrations negatively correlated with 6 MWD ($r = -0.553$, $P < 0.001$), while the correlation coefficient between DKK3 level and 5STS was 0.280 ($P = 0.008$) (Fig. 2b and c). The plasma DKK3 levels and skeletal muscle strength, assessed via quadriceps muscular strength ($r = -0.367$, $P = 0.001$) were also significantly and negatively correlated (Fig. 2d), and the correlation coefficient between DKK3 level and handgrip strength was −0.267 ($P = 0.004$) (Fig. 2e). In addition, the plasma DKK3 levels and skeletal muscle mass, as measured by rectus femoris diameter ($r = -0.454$, $P < 0.001$) and cross-sectional area ($r = -0.490$, $P < 0.001$), were significantly and negatively correlated (Fig. 2f and g).

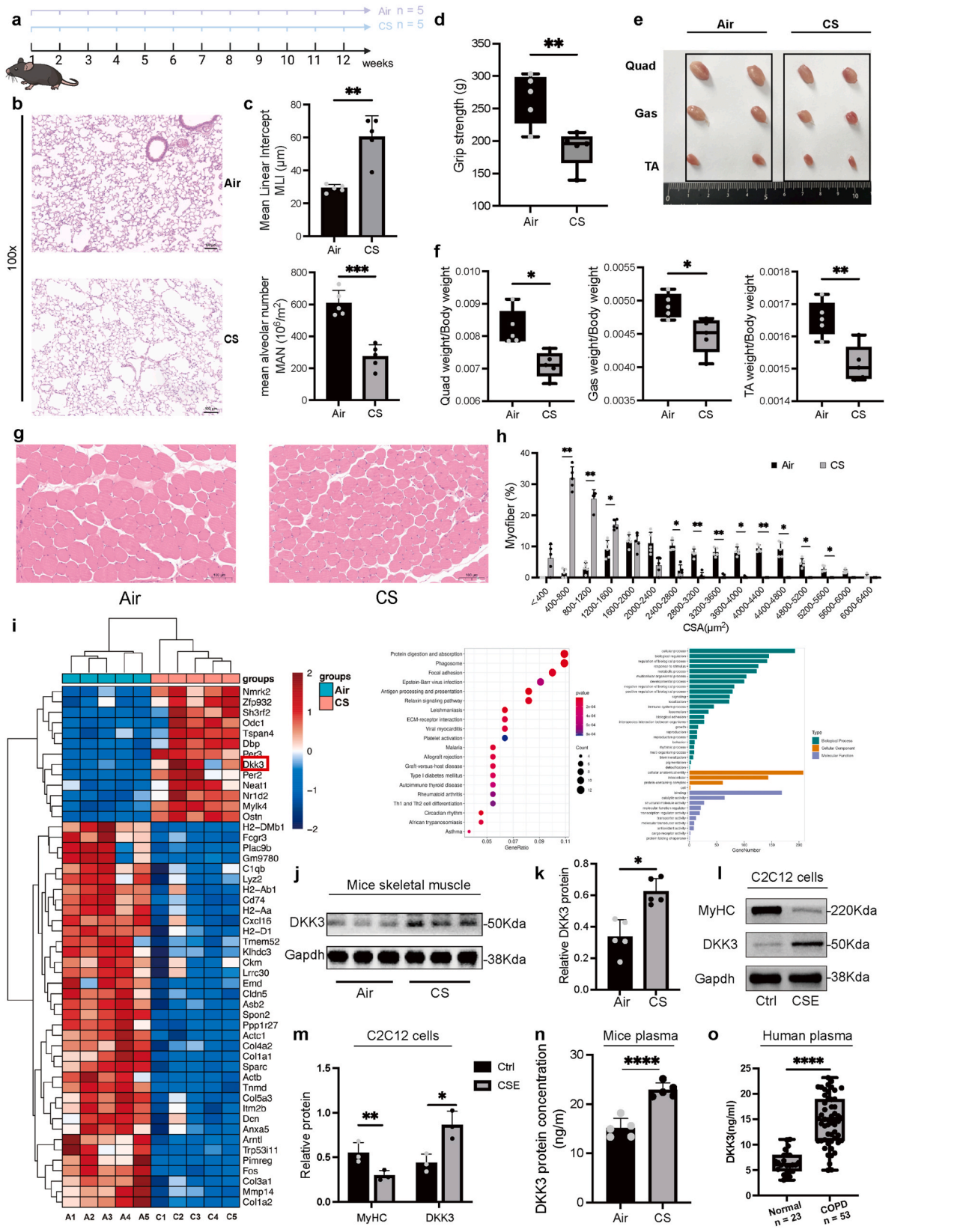

(caption on next page)

Fig. 1. Upregulation of DKK3 in skeletal muscles due to CS-induced muscle atrophy
(a) Schematic diagram illustrating the induction of emphysema and muscle atrophy in male C57BL/6J mice (aged 8–10 weeks) by chronic cigarette smoke (CS) exposure. Each exposure session involved 20 cigarettes (Nicotine 0.8 mg, Tar 10 mg, carbon monoxide 10 mg) twice daily, six days a week, over a 12-week period. (b) Representative H&E staining of lung tissue from CS-exposed and control mice, highlighting the pathological differences. Scale bar: 100 μm. (c) Quantification of mean linear intercept (MLI) and mean alveolar number (MAN) in lung tissues of CS and control mice. (d) Comparison of grip strength between CS-exposed and control mice, showing significant reduction in the former. (e) Representative dissected skeletal muscles among the CS mice and control mice, including Quad (quadriceps), Gas (gastrocnemius) and TA (tibialis anterior). (f) Proportion of Quad, Gast, TA muscle weight in CS-exposed versus control mice. (g, h) Representative H&E staining of TA muscle sections, displaying distribution of myofiber cross-section area (CSA) in CS and control mice. Scale bar: 100 μm. (i) Heatmap of significantly differentially expressed genes in TA muscles, accompanied by Gene Ontology (GO) analysis and Kyoto Encyclopedia of Genes and Genomes. (j, k) Immunoblots and quantification of DKK3 levels in TA muscles of CS and control mice. (l, m) Immunoblots and quantification of whole-cell protein lysates from fully differentiated myotubes treated with CSE for 48h, showing decreased MyHC protein levels and increased expression of DKK3. (n) Elevated plasma levels of DKK3 in CS-exposed mice, as measured by ELISA. (o) Elevated plasma levels of DKK3 in healthy controls (n = 23) and patients with COPD (n = 53), as measured by ELISA. At least five visual fields were randomly selected for each of the biological replicate in pathological analysis. Data are presented as mean ± SD, $^{*}P < 0.05$, $^{**}P < 0.01$, $^{***}P < 0.001$. Two-tailed unpaired Student's *t*-test.

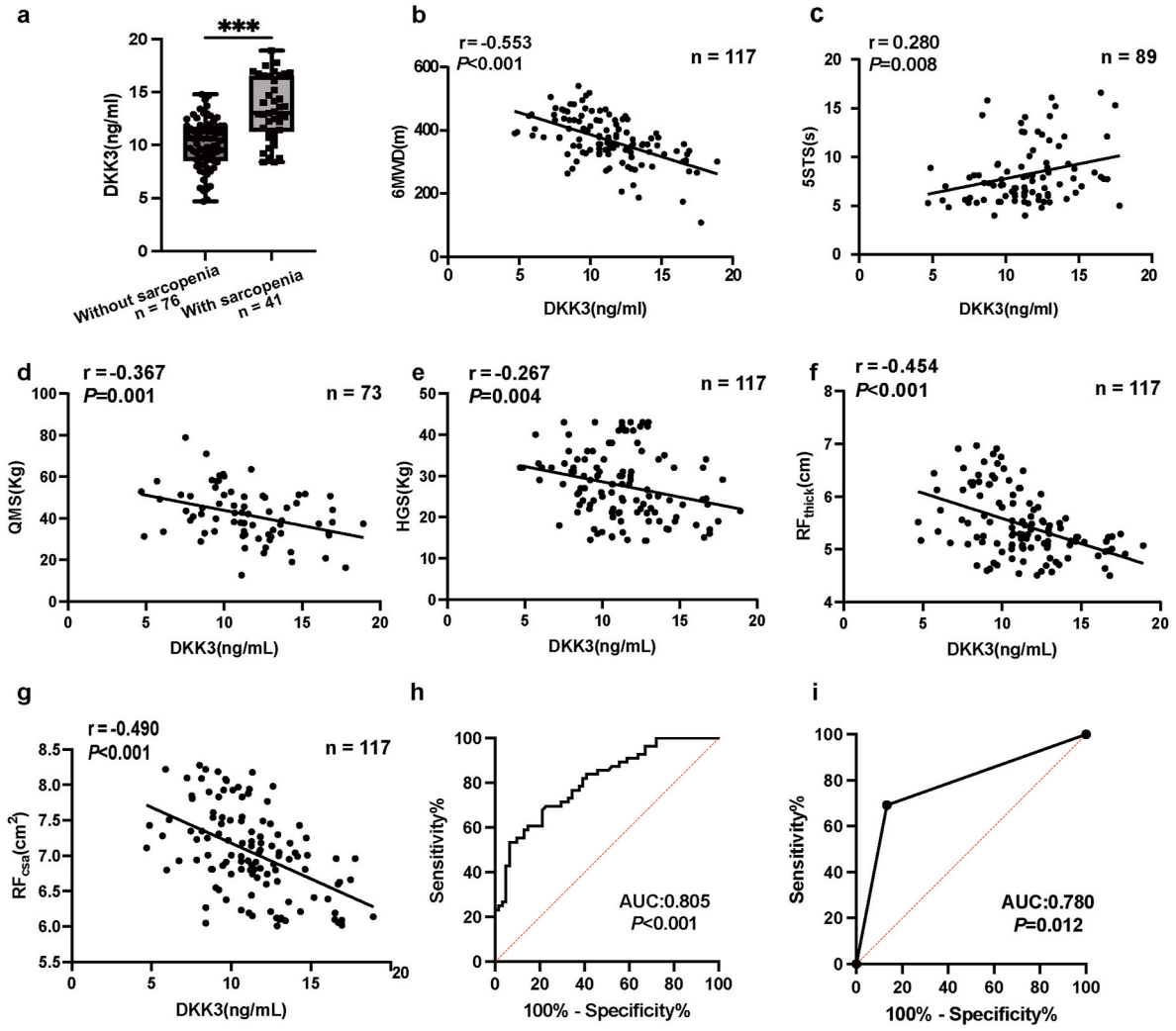

Fig. 2. Elevated Plasma DKK3 Levels Correlate with Disease Severity and Muscle atrophy in Patients with COPD
(a) Plasma DKK3 levels in patients with COPD with and without sarcopenia. (b, c) Correlation between plasma DKK3 levels and exercise tolerance in patients with COPD, assessed by 6-min walk distance (6MWD) and five-time sit-to-stand test (5STS). (d, e) Correlation between plasma DKK3 levels and muscle strength, measured by quadriceps muscular strength (QMS) and handgrip strength (HGS). (f, g) Correlation between plasma DKK3 levels and skeletal muscle mass, measured by rectus femoris diameter (RFthick) and cross-sectional area (RFcsa). (h) Receiver operating characteristic (ROC) curve analysis of plasma DKK3 levels for predicting sarcopenia in patients with COPD in the training set. (i) ROC curve analysis of plasma DKK3 levels for predicting sarcopenia in patients with COPD in the validated set. Data represent mean ± SD, $^{*}P < 0.05$, $^{**}P < 0.01$, $^{***}P < 0.001$.

Next, we investigated the diagnostic efficacy of DKK3 for predicting sarcopenia in paients with COPD. The sensitivity and specificity of plasma DKK3 concentration for predicting sarcopenia in the training set were 53.57 % and 93.44 %, respectively [the cut-off value was 14.32 ng/ml; the Area Under the Curve (AUC) = 0.805, $P < 0.001$] (Fig. 2h). In the validation set, the AUC value for the DKK3 cut-off in identifying sarcopenia in patients with COPD was 0.780 (95 % CI: 0.5968–0.9622, $P = 0.012$). The sensitivity and specificity were 69.23 % (95 % CI: 42.37%–87.32 %) and 86.67 % (95 % CI: 62.12%–97.63 %), respectively. (Fig. 2i). These results suggested that circulating DKK3 level might be a

potential diagnostic marker of sarcopenia in patients with COPD.

3.3. DKK3 overexpression leads to myotube atrophy and mitochondrial dysfunction in cultured myocytes

To investigate the effects of DKK3 on myotube atrophy, we transfected myotubes differentirated from cultured C2C12 cells with pcDNA3.1 plasmids encoding the DKK3 protein (OEDKK3) or empty pcDNA3.1 (pcDNA) as a control. DKK3 overexpression induced significant myotube atrophy compared to the control myotubes, as indicated by MyHC and DAPI immunofluorescence staining (Fig. 3a). DKK3 overexpression also resulted in thinner myotube diameters (Fig. 3b). The MyHC protein levels were decreased, the expressions of atrophy markers and DKK3 were increased in fully-differentiated cells (Fig. 3c–g).

Skeletal mucle mitochondrial dysfunction also involved in the pathophysiology of muscle atrophy in COPD [31,32]. Therefore, we next explored the effect of DKK3 on mitochondrial alterations. Results showed that DKK3 overexpression in C2C12 myocytes resulted in significant mitochondrial dysfunction, with a decreased mitochondrial membrane potential (Fig. 3h and i). DKK3 overexpression significantly suppressed the basal cellular oxygen consumption rate. When mitochondrial ATP synthesis was blocked via oligomycin, reduced ATP-linked oxygen consumption was observed in cells overexpressing DKK3. When the uncoupling agent FCCP was added, impaired maximum oxygen consumption and reserved respiratory capacity was observed in cells overexpressing DKK3 (Fig. 3j and k). In summary, DKK3 overexpression in C2C12 myocytes induceds myotube atrophy, along with significant mitochondrial dysfunction, marked by impaired mitochondrial membrane potential and compromised respiratory capacity.

3.4. DKK3 knockdown rescues CSE-induced C2C12 myotube atrophy and mitochondrial dysfunction in vitro

Next, we probed whether DKK3 knockdown could rescue CSE (cigarette smoke extract)-induced myotube atrophy and mitochondrial dysfunction, we generated DKK3 knockdown C2C12 stable cell line and relative control by stably transduced with lentivirus expressing nonsense shRNA (shNC) or DKK3 targeting shRNA (shDKK3) prior to CSE treatment. DKK3 knockdown rescued CSE-induced myotube atrophy, as indicated by increased myotube diameters (Fig. 4a and b). Western blot analysis of whole-cell protein lysates from fully differentiated myotubes revealed that CSE treatment significantly decreased MyHC protein levels and increased the expression of the muscle atrophy markers Atrogin-1and MuRF1. DKK3 knockdown reversed these changes, resulting in increased MyHC levels and reduced expression of atrophic markers (Fig. 4c–g). Next, we also explored the role of DKK3 knockdown in mitochondrial function. DKK3 knockdown preserved the mitochondrial membrane potential in CSE-treated cells (Fig. 4h and i). In addition, CSE treatment significantly reduced the basal oxygen consumption rate in C2C12 myotubes, though this reduction was rescued by DKK3 knockdown. DKK3 knockdown also improved the ATP-linked oxygen consumption rate and maximal oxygen consumption induced by CSE treatment (Fig. 4j and k). Therefore, the downregulation of DKK3 expression may reverse CSE-induced myotube atrophy and mitochondrial dysfunction in C2C12 myocytes.

3.5. Intramuscular DKK3 knockdown rescues CS-induced skeletal muscle atrophy in mice

Furthermore, we explore the effects of DKK3 in CS-induced muscle atrophy in vivo, adeno-associated virus encoding shRNA against DKK3 (AAV-shDKK3) or scramble shRNA (AAV-shCtrl) were intramuscularly injected into TA muscles of CS mice and controls (Fig. 5a). Skeletal muscles including Quad (quadriceps), Gast (gastrocnemius), TA (tibialis anterior), EDL (extensor digitorum longus), and sol (soleus) were isolated from hind limbs (Fig. 5b). DKK3 expression was reduced in the muscles of the CS mice after AAV-shDKK3 treatment (Fig. 5c). DKK3 knockdown markedly rescued the CS-induced decrease in grip strength (Fig. 5d). The ratios of Quad, Gast, TA muscle to body weights were recorded (Supplemental Fig. 2). The ratios of The reduction of TA muscle weight observed in AAV-shDKK3 CS mice was significantly lower than that observed in shCtrl CS mice (Fig. 5e). The decrease in myofiber diameter in the muscles of CS mice was reversed by DKK3 knockdown, no significant differences were observed in the non-smoking control groups (Fig. 5f and h). The distribution and quantification of myofiber size in the TA muscles of CS mice treated with AAV-shDKK3 shifted towards larger CSA compared to treated with scrambled AAV-shCtrl (Fig. 5g and h). The increased protein levels of Atrogin-1 and MuRF1 induced by CS were significantly reduced in the TA muscles of mice treated with AAV-shDKK3 (Fig. 5i–k). No significant differences were observed between control mice treated with scrambled shRNA or shRNA against DKK3. Intramuscular DKK3 knockdown effectively mitigates CS-induced muscle degradation in mice, as evidenced by improved muscle strength, preserved muscle mass, and reduced expression of muscle atrophy markers.

3.6. DKK3-mediated paracrine activity contributes to C2C12 myotube atrophy in vitro

Muscle has recently been recognized as a key endocrine organ because of its ability to produce and secrete myokines. DKK3, acting as a secreted protein, induces muscle atrophy through paracrine or autocrine mechanisms [16]. We transfected differentiated myotubes with pcDNA3.1, plasmids encoding the DKK3 protein (OEDKK3), and harvested the conditioned medium (CM) to treat myotubes derived from C2C12 cells. CM from myotubes transfected with empty pcDNA3.1 (pcDNA) served as a control (Fig. 6a). The DKK3 protein levels were increased in OE-DKK3 CM (Fig. 6b and Supplemental Fig. 3). The myotubes treated with OEDKK3 CM were significantly thinner than those treated with control CM (Fig. 6c–d). The MyHC protein levels were decreased in whole-cell lysates from myotubes treated with OEDKK3 CM and the expressions of the atrophy markers Atrogin-1 and MuRF1 were increased (Fig. 6e–h). Furthermore, we evaluated the therapeutic potential of DKK3 antibodies for CSE-induced myotube atrophy. We administered CSE combined with a monoclonal antibody against DKK3 (mAb-DKK3, 60 ng/mL) to C2C12 myotubes. The myotube size and MyHC protein levels were also restored after treatment with DKK3 monoclonal antibodies (Fig. 6i–l). In conclusion, DKK3 induced myotube atrophy through autocrine and paracrine signaling, an effect that can be counteracted by monoclonal antibodies.

3.7. DKK3 physically interacts with CKAP4 to induce skeletal muscle atrophy in vitro

To explore the mechanism by which DKK3 mediates myofiber atrophy in C2C12 myotubes, we performed an immunoprecipitation of endogenous DKK3 from C2C12 cells, followed by mass spectrometry analysis. This procedure identified 254 interacting proteins (Fig. 7a). Considering that DKK3 is a secretory protein, we focused on proteins located at the cell surface. Out of the 27 plasma membrane proteins identified, 6 were located on the cell surface. Among these, cytoskeleton-associated protein 4 (CKAP4) was of particular interest (Fig. 7b). The immunoprecipitation of endogenous DKK3 led to the co-precipitation of CKAP4, and the immunoprecipitation of endogenous CKAP4 led to the co-precipitation of DKK3 (Fig. 7c).

To verify the regulatory effect of DKK3 dependenting on CKAP4 on myofiber atrophy, we transiently transfected C2C12 myotubes with siRNA targeting CKAP4 before treating with rhDKK3. The myofiber atrophy effect induced by rhDKK3 was altered by suppressing CKAP4 expression, as demonstrated by increased protein levels of MyHC, decreased expressions of Atrogin-1 and MuRF1 and suppressed expression of CKAP4 (Fig. 7d–h). CKAP4 knockdown attenuated the rhDKK3-

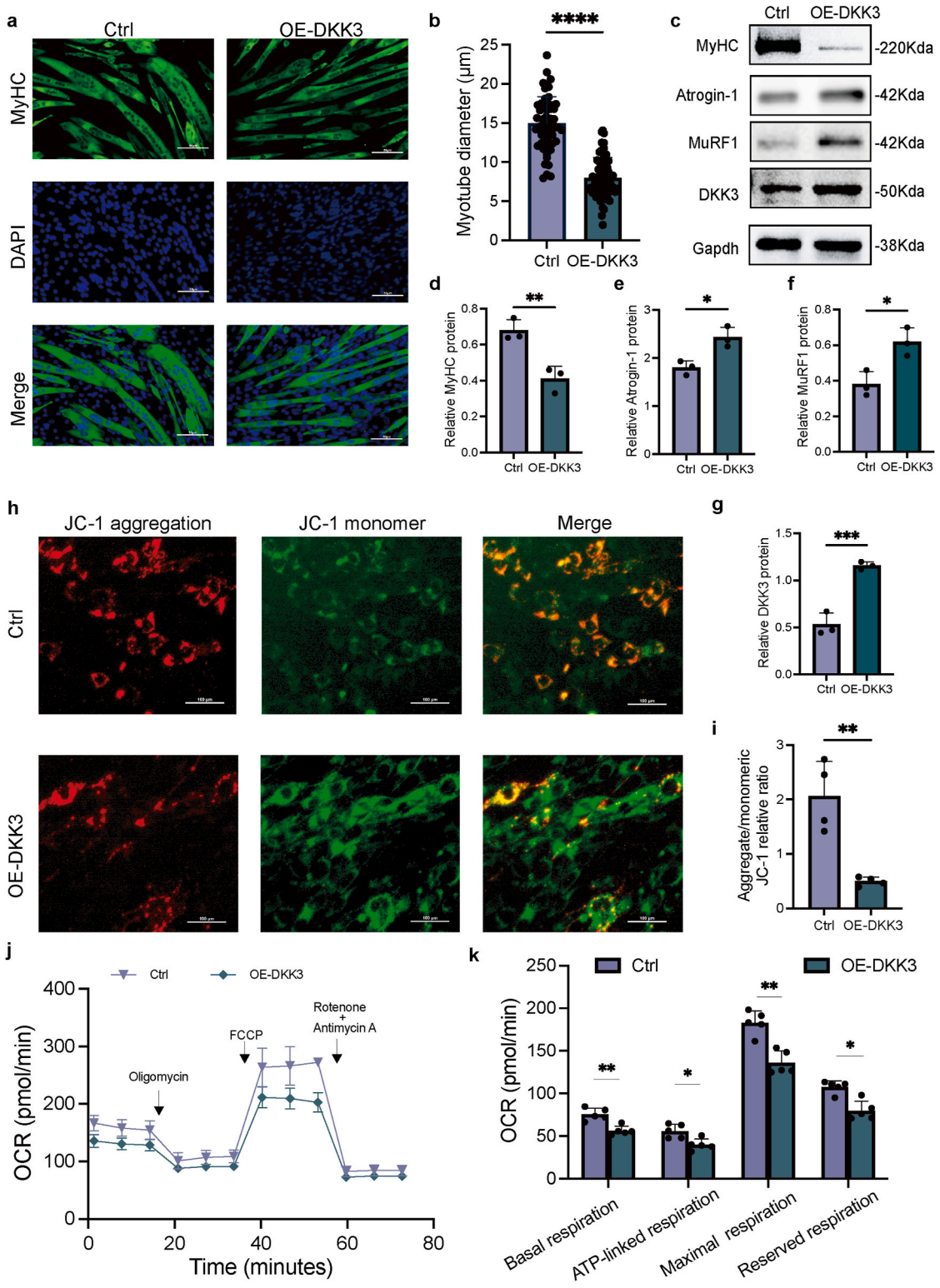

Fig. 3. DKK3 over-expression leads to myotube atrophy and mitochondrial dysfunction in cultured myocytes
(a) Representative immunofluorescence images of MyHC (green) and DAPI (blue) in C2C12 myotubes transfected with pcDNA or DKK3 plasmid. Scale bar: 50 μm. (b) Quantification of the average diameters of the control myotubes or DKK3 over-expressing myotubes. (c–g) Immunoblots and quantification of whole-cell protein lysates from fully differentiated myotubes showing decreased MyHC protein levels, increased expression of muscle atrophy markers Atrogin-1 and MuRF1, and increased DKK3 protein level in DKK3-overexpressed cells compared to controls. The data represent three independent experiments. (h) Representative immunofluorescence images of JC-1 staining in C2C12 cells transfected with control or DKK3 plasmids. Scale bar: 100 μm. (i) Quantitative results show the ratio of JC-1 aggregate (red) to monomeric (green) forms, indicating a significant decrease in mitochondrial membrane potential in DKK3-overexpressed myotubes. At least five fields were randomly selected for each of the four biological replicates in immunofluorescence analysis. (j) Cellular oxygen consumption rate (OCR) in C2C12 cells transfected with control or DKK3 plasmids. (k) Basal, ATP-linked, maximal and reserved OCR were quantified and analyzed. DKK3 over-expression significantly suppresses basal OCR and ATP-linked OCR, impaired maximum and reserved OCR. Data are presented as mean ± SD, $^{*}P < 0.05$, $^{**}P < 0.01$, $^{***}P < 0.001$. Two-tailed unpaired Student's *t*-test. (For interpretation of the references to color in this figure legend, the reader is referred to the Web version of this article.)

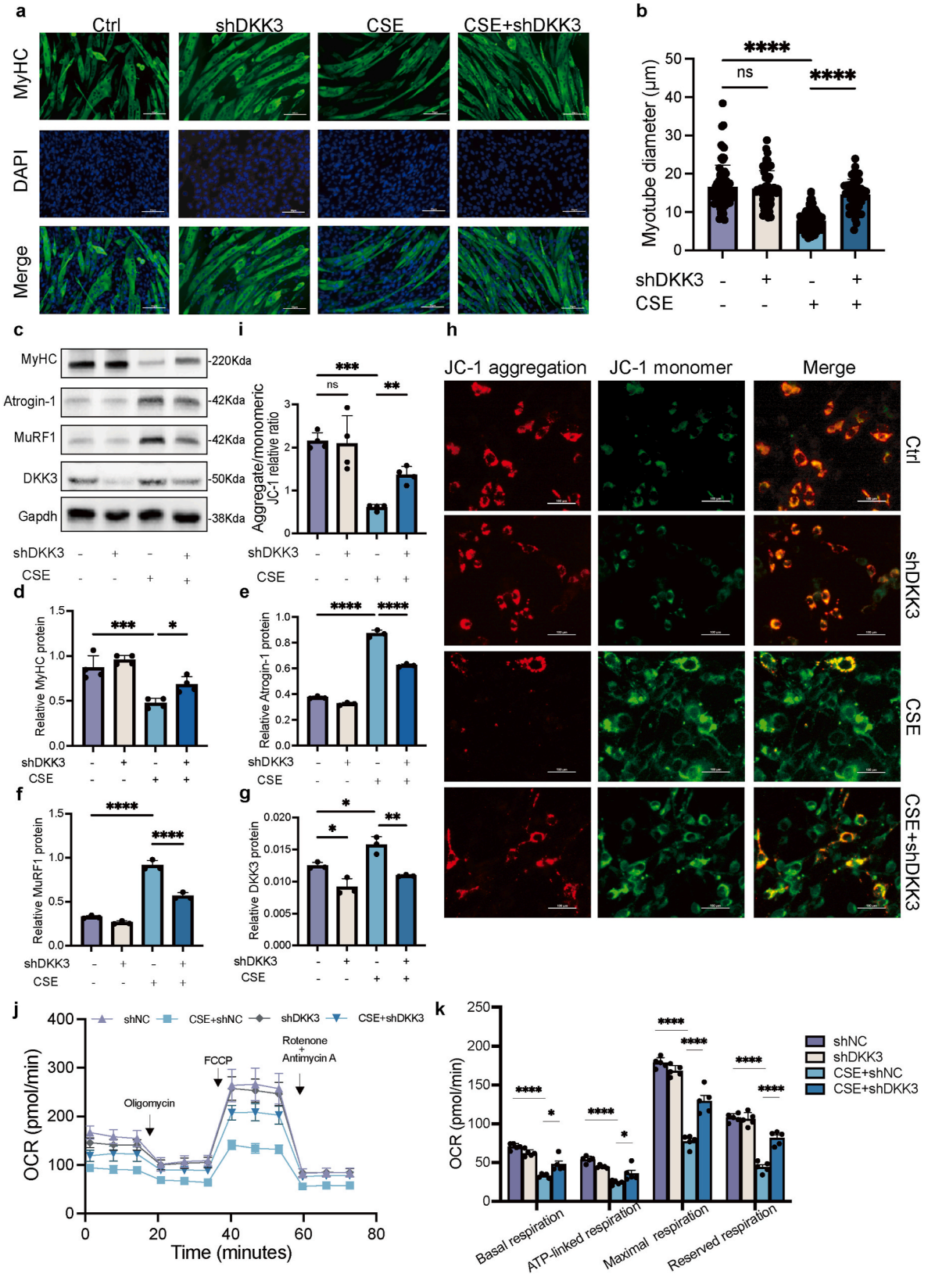

(caption on next page)

Fig. 4. DKK3 knockdown rescues CSE-induced myotube atrophy and mitochondrial dysfunction
(a) Representative immunofluorescence images of MyHC and DAPI in C2C12 myotubes stably transduced with shNC or shDKK3 lentivirus prior to CSE treatment. Scale bar: 50 μm. (b) Quantification of the average diameters of myotubes differentiated from shNC or shDKK3 C2C12 cells with or without CSE-treatment. At least three fields were randomly selected for each of the five biological replicates. (c–g) Immunoblots and quantification of relative MyHC protein levels, muscle atrophy markers Atrogin-1 and MuRF1 and DKK3 protein levels in whole-cell protein lysates from fully differentiated myotubes under different conditions. The data represent three independent experiments. (h) Representative immunofluorescence images of JC-1 staining in C2C12 cells transfected with shNC or shDKK3 prior to CSE treatment. DKK3 knockdown preserves mitochondrial membrane potential in CSE-treated cells. Scale bar: 100 μm. (i) Quantitative results showing the ratio of JC-1 aggregate (red) to monomeric (green) forms. At least five fields for each of the four biological replicates per group. (j) Cellular oxygen consumption rate (OCR) in C2C12 cells transfected with shNC or shDKK3 prior to CSE treatment. (k) Basal, ATP-linked, maximal and reserved OCR were quantified and analyzed. Data represent mean ± SD, $^{*}P < 0.05$, $^{**}P < 0.01$, $^{***}P < 0.001$. One-way ANOVA with multiple comparisons. (For interpretation of the references to color in this figure legend, the reader is referred to the Web version of this article.)

induced increase in ubiquitination of total proteins from C2C12 myotubes (Supplemental Fig. 3). CKAP4 knockdown prior to rhDkk3 administration alleviated the DKK3-induced decrease in mitochondrial membrane potential (Fig. 3i and j). These results suggested that CKAP4 mediatesd the effect of DKK3 on myofiber atrophy and mitochondrial dysfunction in myotubes.

4. Disscusion

The findings of this study indicate that plasma DKK3 levels can be used to identify sarcopenia in patients with COPD. A cutoff value for plasma DKK3 levels was determined and confirmed using a validation set. DKK3 is a secreted factor produced by skeletal muscles that acts in autocrine and paracrine manners, interacting with the cell surface-activated receptor CKAP4 to induce mitochondrial dysfunction and myotube atrophy. Inhibition of DKK3 via genetic ablation resulted in preventive functions against CS-induced skeletal muscle dysfunction, suggesting that DKK3 is a potential target for the diagnosis and treatment of sarcopenia in patients with COPD. Previous studies by Yin, J et al. [30] have identified DKK3 as a key regulator in muscle atrophy, demonstrating that DKK3 activates the transcription of E3 ubiquitin ligases, leading to muscle degradation. Our results were consistent with these findings. Specifically, our study highlights that DKK3 induces muscle atrophy and mitochondrial dysfunction through its interaction with the cell surface receptor CKAP4 in an autocrine and paracrine manner. Additionally, our research investigated the underlying mechanisms of DKK3-mediated muscle atrophy within the context of a CS disease model, which is different from the study of Yin, J. et al. in the age-related muscle atrophy.

DKK3 is an emerging biomarker that has been implicated in several diseases [33]. Urinary DKK3 levels have the potential to be utilized as a biomarker for tracking the progression of kidney disease and assessing intervention outcomes [34–36] and may be a biomarker for the early identification of silent progressive chronic kidney disease and adverse outcomes in patients with COPD [37]. In this study, the plasma DKK3 levels were found to be associated with the quality and quantity of skeletal muscle in patients with COPD. Increased plasma DKK3 levels were associated with more severe skeletal muscle dysfunction in patients with COPD, which is consistent with a previous report [38]. Our results showed that the sensitivity and specificity of plasma DKK3 concentration for predicting sarcopenia in the training set were 53.57 % and 93.44 %, respectively. Although DKK3 has limitations in ruling out sarcopenia, as indicated by its lower negative predictive value (NPV = 78.9 %), its positive predictive value (PPV = 81.5 %) remains clinically significant (Supplemental Table 3). A positive DKK3 result strongly suggests sarcopenia, making it valuable for confirming high-risk individuals and distinguishing patients with COPD and sarcopenia. Additionally, detecting plasma levels of DKK3 is more accessible and streamlined compared to conventional methods, especially in settings with limited access to traditional diagnostic devices, such as dual-energy X-ray absorptiometry (DXA) or bioimpedance analysis and dynamometer. Thus, DKK3 complements traditional methods, providing a more comprehensive diagnostic perspective. Combining it with other clinical assesments is recommended to improve overall diagnostic accuracy.

Mitochondria are the main organelles that regulate energy metabolism in skeletal muscles, and mitochondrial dysfunction and the resulting increased breakdown of muscle proteins are hallmarks of sarcopenia [39,40]. Recent studies have revealed altered mitochondrial numbers and functions in the skeletal muscles of patients with COPD ([41,42]). Improving mitochondrial function may improve skeletal muscle function in patients with COPD. In this study, DKK3 was involved in CS-induced skeletal muscle dysfunction via the induction of mitochondrial dysfunction and myotube atrophy. The inhibition of DKK3 via genetic ablation or pharmacologic depletion using monoclonal antibodies prevented CS-induced skeletal muscle dysfunction. Overall, these results suggest that DKK3 is a potential therapeutic target for skeletal muscle dysfunction in patients with COPD.

In addition, DKK3 physically interacts with CKAP4 to activate downstream signaling cascades, leading to skeletal muscle dysfunction. CKAP4 is a non-glycosylated type II transmembrane protein that functions as a cell surface-activated receptor [43,44] and is an important regulator of carcinogenesis in several types of cancer (including pancreatic cancer [45] and cervical cancer) by interacting with ligands such as DKK1 and APF(44). Therefore, targeting CKAP4 may be a potential strategy for cancer treatment [43]. However, the function of CKAP4 in skeletal muscle remains unclear. In this study, DKK3-mediated mitochondrial dysfunction and myotubular atrophy in skeletal muscle cells are dependent on its binding to CKAP4. Overall, these results suggest that CKAP4, a receptor for DKK3, plays a role in CS-induced skeletal muscle dysfunction.

Recently, there has been an increasing emphasis on sex differences in disease models. Previous studies have shown that estrogen may partly account for women's higher susceptibility to tobacco's harmful effects [46,47]. Compared with male human smokers, female human smokers had significantly thicker airway walls. In animal models, chronic smoke exposure increased small airway remodeling in female mice compared with male mice using the smoke exposure model of COPD [48]. Moreover, the influence of estrogen on skeletal muscle has become evident across human, animal, and cell-based studies. Estrogen has been shown to exert a significant influence on skeletal muscle across human, animal, and cell-based studies. Their beneficial effects include reducing muscle injury and facilitating repair through mechanisms such as the preservation of satellite cell function, enhancement of membrane stability, and potential antioxidant properties [49]. These results suggest the potentially different pathophysiological mechanisms of COPD and sarcopenia between the sexes, indicating the need for sex-specific consideration. However, there is a higher historical prevalence among men in COPD, which has been linked to greater smoking rates in this population, as acknowledged in the GOLD 2024 report, though the report also highlights that the gender gap in COPD prevalence is narrowing due to shifts in smoking patterns [50]. Furthermore, smoke exposure-induced muscle atrophy models were based on male mice in previous studies [28,51,52]. Given these findings and to align with previous studies, we established a smoke exposure-induced muscle atrophy model in male mice to ensure consistency.

Our findings showed that CS exposure significantly increased DKK3 mRNA levels in the skeletal muscles of CS-exposed mice, which indicated aberrant transcription of DKK3. Benzo(*a*)pyrene (BaP), one of the

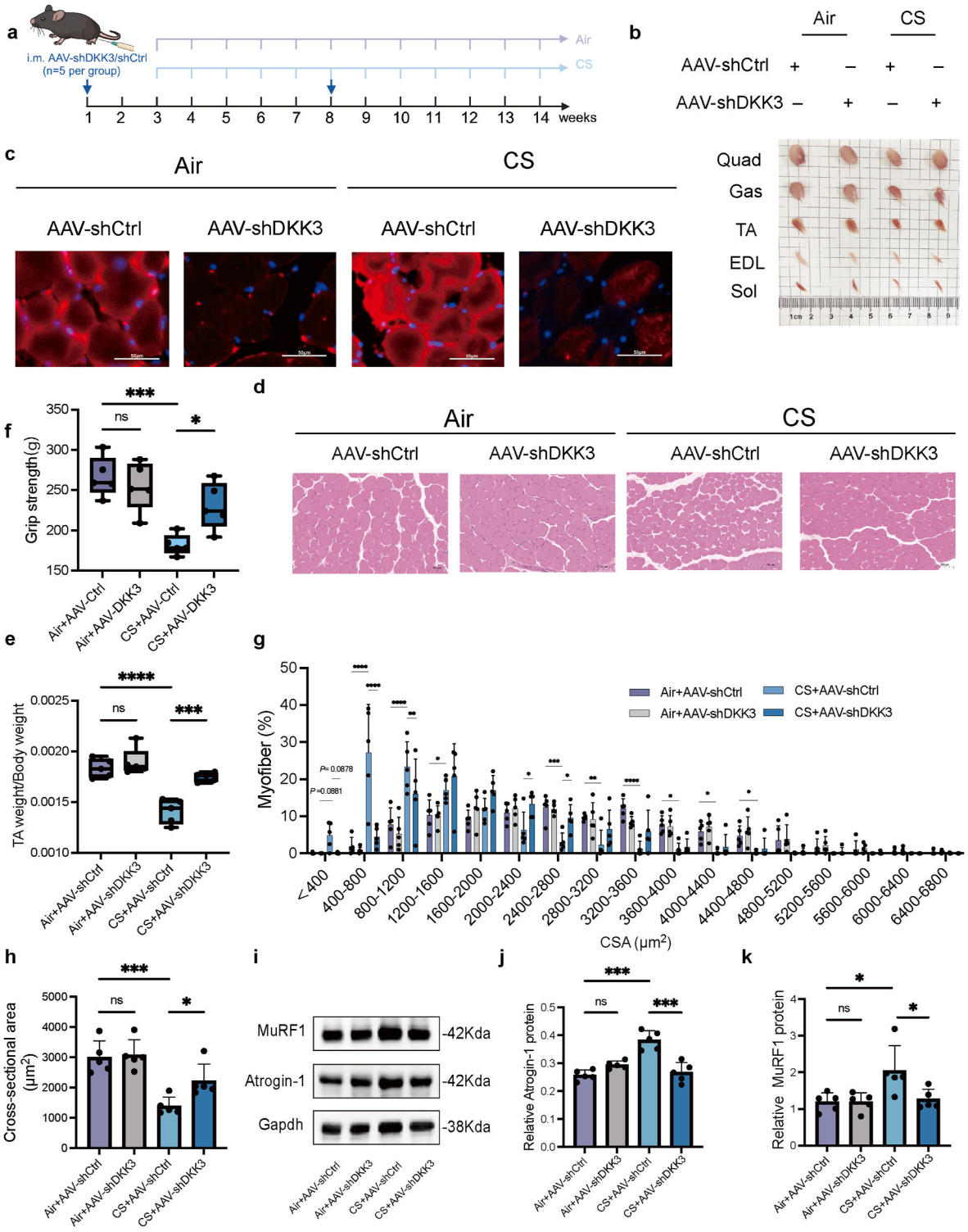

Fig. 5. Intramuscular DKK3 knockdown rescues CS-induced skeletal muscle atrophy in mice

(a) Schematic representation of intramuscular injection of AAV-shDKK3 or AAV-shCtrl into TA muscles of CS and control mice. (b) Representative dissected skeletal muscles among the four groups: CS mice with AAV-shDKK3, CS mice with AAV-shCtrl, control mice with AAV-shDKK3, and control mice with AAV-shCtrl, including Quad (quadriceps), Gast (gastrocnemius), TA (tibialis anterior), EDL (extensor digitorum longus), and sol (soleus); (c) Representative immunofluorescence images of DKK3 (red) and DAPI (blue) in TA muscles, confirming efficient knockdown of DKK3 expression by AAV-shDKK3. Scale bar: 50 μm. (d) Quantification of grip strength in CS and control mice treated with AAV-shDKK3 or AAV-shCtrl (n = 5 per group, 5 measuremeants per mouse) (e) Comparison of the proportion of TA muscle weights among the four groups (n = 5 per group). (f) Representative H&E staining of TA muscle sections showing myofiber cross-sectional area (CSA) from the four groups. Scale bar: 100 μm. (g, h) The distribution and quantification of myofiber CSA in TA muscles from the different groups (n = 5 per group, at least 5 fields per mouse). (i–k) Immunoblots and quantification of relative Atrogin-1 and MuRF1 protein levels in TA muscle lysates from the four groups (n = 5 per group). Data represent mean ± SD, $^{*}P < 0.05$, $^{**}P < 0.01$, $^{***}P < 0.001$. One-way ANOVA with multiple comparisons. (For interpretation of the references to color in this figure legend, the reader is referred to the Web version of this article.)

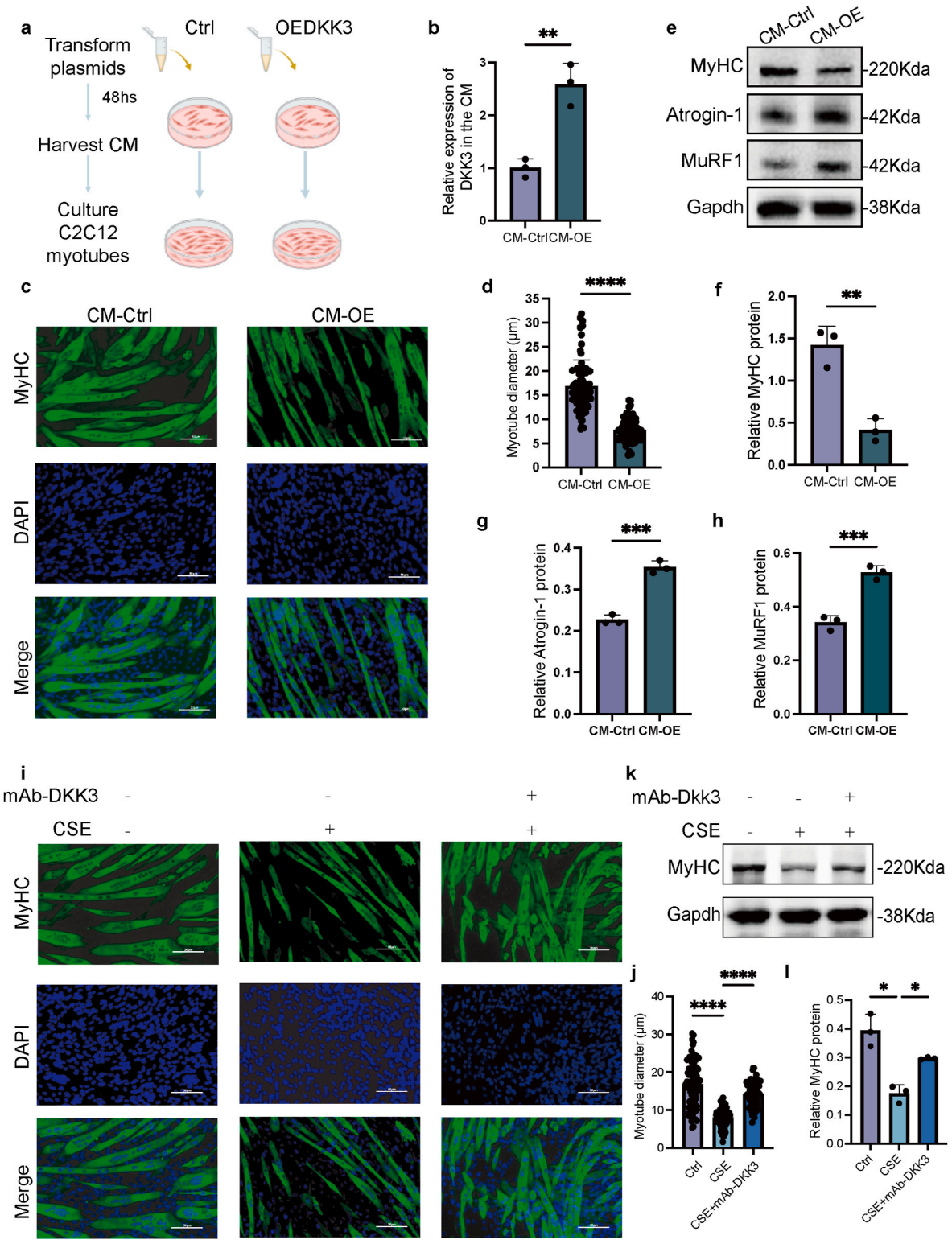

Fig. 6. DKK3-mediated paracrine effects contribute to myotube atrophy

(a) Schematic outline of conditioned medium (CM) harvested from C2C12 myotubes transfected with pcDNA3.1 plasmids encoding DKK3 (OEDKK3) or empty pcDNA3.1 (control). The CM was used to treat myotubes derived from C2C12 cells. (b) Relative fold change of DKK3 expression level in the CM from control and OEDKK3 C2C12 myotubes. (c) Representative immunofluorescence images of MyHC (green) and DAPI (blue) in myotubes treated with CM harvested from OEDKK3 or control myotubes. Scale bar: 50 μm. (d) Quantification of the average diameters of myotubes of each group. (e–h) Immunoblots and quantification of relative MyHC and muscle atrophy markers protein levels in the total cell protein lysates from myotubes as described in b. (i) Representative immunofluorescence images of MyHC (green) and DAPI (blue) in myotubes subjected to CSE alone or in combination with monoclonal antibody against DKK3 (mAb-DKK3, 60 ng/mL), Scale bar: 50 μm. (j) Quantification of the average diameters of myotubes of each group. (k) Immunoblot analysis and quantification of MyHC in total cell protein lysates from myotubes treated with CSE alone or in combination with mAb-DKK3. Data represent mean ± SD, $^{*}P < 0.05$, $^{**}P < 0.01$, $^{***}P < 0.001$. One-way ANOVA with multiple comparisons. (For interpretation of the references to color in this figure legend, the reader is referred to the Web version of this article.)

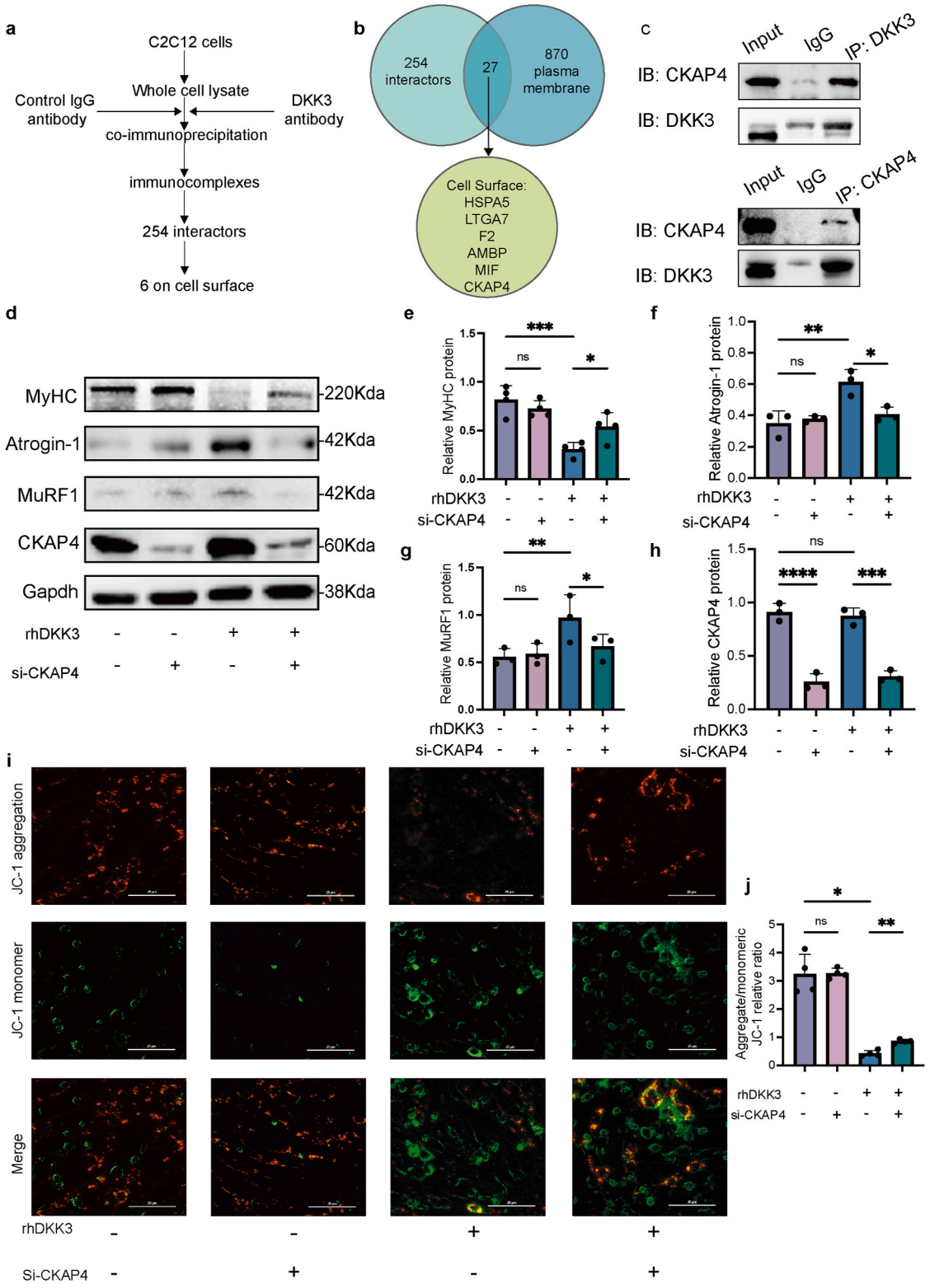

Fig. 7. DKK3 physically interacts with CKAP4 to induce skeletal muscle atrophy

(a) Schematic experimental procedure depicting the workflow for identifying DKK3-interacting proteins via immunoprecipitation and mass spectrometry in C2C12 cells. (b) Venn diagram analysis showing the overlap among DKK3-interacting proteins, plasma membrane proteins, and cell surface proteins. (c) Co-immunoprecipitation experiments confirmed the physical interaction between DKK3 and CKAP4. (d–h) Representative immunoblots and quantification showing MyHC protein levels, muscle atrophy markers Atrogin-1 and MuRF1 and CKAP4 protein in C2C12 myotubes treated with rhDKK3, with or without CKAP4 knockdown. (i) JC-1 staining demonstrating that CKAP4 knockdown mitigates the DKK3-induced reduction in mitochondrial membrane potential. Scale bar: 5 μm. (j) Quantitative results of JC-1 aggregate (red)/monomeric (green) forms are shown. At least five fields were randomly selected for each of the four biological replicates. Data represent mean ± SD, $*P < 0.05$, $**P < 0.01$, $***P < 0.001$. One-way ANOVA with multiple comparisons. (For interpretation of the references to color in this figure legend, the reader is referred to the Web version of this article.)

main tobacco carcinogens in tobacco smoke, activates aryl hydrocarbon receptor (AhR) and increases the PD-L1 expression in mRNA level [53]. The AhR is a ligand-activated transcription factor that activates detoxifying pathways with numerous exogenous ligands, including tobacco smoke. Previous study has shown that smoke exposure increased muscle AhR signaling in mouse and human patient specimens, as well as in CSE-treated C2C12 myotubes, and caused mitochondrial impairments, and induced an AHR-dependent myotube atrophy [51,52]. Besides, the association of the Wnt-genes (DKK4, DKK3, DKK2 et al.) and AhR was reported to affect the susceptibility to lung cancer, which suggested the potential association between DKK3 and AhR. These data indicate that AhR plays a crucial role in CS-induced skeletal muscle dysfunction and may be involved in regulating DKK3 expression.

This study is not without limitations. First, the CSE model was used in in vitro experiments to represent COPD-related sarcopenia. Pro-inflammatory cytokines are closely linked to the extrapulmonary comorbidities of COPD, with leakage from the inflamed lung being a crucial mechanism. Given the cross-sectional nature of this study, additional prospective cohort studies are necessary to confirm the potential of DKK3 as a predictor of sarcopenia risk. Furthermore, our study primarily focused on the genetic inhibition of DKK3, both in vivo and in vitro while inhibiting DKK3 pharmacologically using monoclonal antibodies was explored only in CSE-treated C2C12 myotubes and not investigated in CS mice model. Future research incorporating these in vivo evaluations would be essential for a comprehensive assessment of the therapeutic potential of DKK3 inhibition in CS mice model.

5. Conclusion

In conclusion, a cut-off value for plasma DKK3 levels that identifies sarcopenia in patients with COPD was determined and validated in this study. DKK3 is secreted by skeletal muscle tissue and exerts its effects through autocrine and paracrine pathways via interactions with CKAP4 to induce mitochondrial dysfunction and myotube atrophy. Inhibiting DKK3 genetically prevents CS-induced skeletal muscle dysfunction. These findings highlight the potential of DKK3 as a diagnostic marker and therapeutic target for sarcopenia in patients with COPD.

CRediT authorship contribution statement

Zilin Wang: Writing – original draft, Visualization, Methodology, Data curation. **Mingming Deng:** Writing – original draft, Methodology, Data curation. **Weidong Xu:** Software, Methodology, Formal analysis. **Chang Li:** Methodology, Formal analysis, Data curation. **Ziwen Zheng:** Software, Formal analysis. **Jiaye Li:** Methodology, Formal analysis, Data curation. **Liwei Liao:** Methodology, Formal analysis, Data curation. **Qin Zhang:** Methodology, Formal analysis. **Yiding Bian:** Writing – review & editing, Formal analysis. **Ruixia Li:** Resources, Data curation. **Jinrui Miao:** Supervision, Methodology, Data curation. **Kai Wang:** Resources, Data curation. **Yan Yin:** Supervision, Resources. **Yanxia Li:** Supervision, Resources. **Xiaoming Zhou:** Validation, Data curation. **Gang Hou:** Writing – review & editing, Validation, Supervision, Resources, Project administration, Conceptualization.

Informed consent

Informed consent was obtained for experimentation with human subjects.

Funding

This research was supported by National High Level Hospital Clinical Research Funding (2024-NHLHCRF-JBGS-WZ-05), National Natural Science Foundation of China (82300053, 82470039, 82400041, 82400042), China Postdoctoral Science Foundation (2024M753704, 2024M753705), National High Level Hospital Clinical Research Funding (2022-NHLHCRF-LX-01), CAMS Institute of Respiratory Medicine Grant for Young Scholars (2023-ZF-74), the Fundamental Research Funds for the Central Universities (3332024101).

Declaration of competing interest

The authors declare that they have no known competing financial interests or personal relationships that could have appeared to influence the work reported in this paper.

Appendix A. Supplementary data

Supplementary data to this article can be found online at https://doi.org/10.1016/j.redox.2024.103434.

Data availability

Data will be made available on request.

References

[1] K.F. Rabe, H. Watz, Chronic obstructive pulmonary disease, Lancet (London, England) 389 (10082) (2017 May 13) 1931–1940. PubMed PMID: 28513453. Epub 2017/05/18. eng.
[2] L. Vanfleteren, M.A. Spruit, E.F.M. Wouters, F.M.E. Franssen, Management of chronic obstructive pulmonary disease beyond the lungs, Lancet Respir. Med. 4 (11) (2016 Nov) 911–924. PubMed PMID: 27264777. Epub 2016/11/02. eng.
[3] W. Sepúlveda-Loyola, C. Osadnik, S. Phu, A.A. Morita, G. Duque, V.S. Probst, Diagnosis, prevalence, and clinical impact of sarcopenia in COPD: a systematic review and meta-analysis, Journal of cachexia, sarcopenia and muscle 11 (5) (2020 Oct) 1164–1176. PubMed PMID: 32862514. PMCID: PMC7567149. Epub 2020/08/31. eng.
[4] D. Liu, S. Wang, S. Liu, Q. Wang, X. Che, G. Wu, Frontiers in sarcopenia: advancements in diagnostics, molecular mechanisms, and therapeutic strategies, Mol. Aspect. Med. 97 (2024 Apr 6) 101270. PubMed PMID: 38583268. Epub 20240406. eng.
[5] P. Limpawattana, P. Inthasuwan, S. Putraveephong, W. Boonsawat, D. Theerakulpisut, K. Sawanyawisuth, Sarcopenia in chronic obstructive pulmonary disease: a study of prevalence and associated factors in the Southeast Asian population, Chron. Respir. Dis. 15 (3) (2018 Aug) 250–257. PubMed PMID: 29186972. PMCID: PMC6100162. Epub 2017/12/01. eng.
[6] J.J. McCarthy, K.A. Esser, Anabolic and catabolic pathways regulating skeletal muscle mass, Curr. Opin. Clin. Nutr. Metab. Care 13 (3) (2010 May) 230–235. PubMed PMID: 20154608. PMCID: PMC2877703. Epub 2010/02/16. eng.
[7] L. Han, P. Li, Q. He, C. Yang, M. Jiang, Y. Wang, et al., Revisiting skeletal muscle dysfunction and exercise in chronic obstructive pulmonary disease: emerging significance of myokines, Aging Dis. 15 (6) (2023 Dec 7) 2453–2469. PubMed PMID: 38270119. Epub 2024/01/25. eng.
[8] R.M. Abdulai, T.J. Jensen, N.R. Patel, M.I. Polkey, P. Jansson, B.R. Celli, et al., Deterioration of limb muscle function during acute exacerbation of chronic obstructive pulmonary disease, Am. J. Respir. Crit. Care Med. 197 (4) (2018 Feb 15) 433–449. PubMed PMID: 29064260. PMCID: PMC5821903. Epub 2017/10/25. eng.
[9] H. Degens, G. Gayan-Ramirez, H.W. van Hees, Smoking-induced skeletal muscle dysfunction: from evidence to mechanisms, Am. J. Respir. Crit. Care Med. 191 (6) (2015 Mar 15) 620–625. PubMed PMID: 25581779. Epub 2015/01/13. eng.
[10] G. Haji, C.H. Wiegman, C. Michaeloudes, M.S. Patel, K. Curtis, P. Bhavsar, et al., Mitochondrial dysfunction in airways and quadriceps muscle of patients with chronic obstructive pulmonary disease, Respir. Res. 21 (1) (2020 Oct 12) 262. PubMed PMID: 33046036. PMCID: PMC7552476. Epub 2020/10/14. eng.
[11] J.R. Gifford, J.D. Trinity, G. Layec, R.S. Garten, S.Y. Park, M.J. Rossman, et al., Quadriceps exercise intolerance in patients with chronic obstructive pulmonary disease: the potential role of altered skeletal muscle mitochondrial respiration, J. Appl. Physiol. 119 (8) (2015 Oct 15) 882–888. PubMed PMID: 26272320. PMCID: PMC4610006. Epub 2015/08/15. eng.
[12] P.A. Leermakers, A. Schols, A.E.M. Kneppers, M. Kelders, C.C. de Theije, M. Lainscak, et al., Molecular signalling towards mitochondrial breakdown is enhanced in skeletal muscle of patients with chronic obstructive pulmonary disease (COPD), Sci. Rep. 8 (1) (2018 Oct 9) 15007. PubMed PMID: 30302028. PMCID: PMC6177478. Epub 2018/10/12. eng.
[13] P.A. Leermakers, H.R. Gosker, Skeletal muscle mitophagy in chronic disease: implications for muscle oxidative capacity? Curr. Opin. Clin. Nutr. Metab. Care 19 (6) (2016 Nov) 427–433. PubMed PMID: 27537277. Epub 2016/10/18. eng.
[14] E. Marzetti, R. Calvani, M. Cesari, T.W. Buford, M. Lorenzi, B.J. Behnke, et al., Mitochondrial dysfunction and sarcopenia of aging: from signaling pathways to clinical trials, Int. J. Biochem. Cell Biol. 45 (10) (2013 Oct) 2288–2301. PubMed PMID: 23845738. PMCID: PMC3759621. Epub 2013/07/13. eng.
[15] L. Larsson, H. Degens, M. Li, L. Salviati, Y.I. Lee, W. Thompson, et al., Sarcopenia: aging-related loss of muscle mass and function, Physiol. Rev. 99 (1) (2019 Jan 1) 427–511. PubMed PMID: 30427277. PMCID: PMC6442923 drugs are held by Mayo

Clinic. This work has been revised by the Mayo Clinic Conflict of Interest Review Board and was conducted in compliance with Mayo Clinic conflict of interest policies. No other conflicts of interest, financial or otherwise, are declared by the authors. Epub 2018/11/15. eng.
[16] C. Niehrs, Function and biological roles of the Dickkopf family of Wnt modulators, Oncogene 25 (57) (2006 Dec 4) 7469–7481. PubMed PMID: 17143291. eng.
[17] M.V. Semënov, K. Tamai, B.K. Brott, M. Kühl, S. Sokol, X. He, Head inducer Dickkopf-1 is a ligand for Wnt coreceptor LRP6, Curr. Biol. : Cailiao Baohu 11 (12) (2001 Jun 26) 951–961. PubMed PMID: 11448771. Epub 2001/07/13. eng.
[18] B. Mao, W. Wu, G. Davidson, J. Marhold, M. Li, B.M. Mechler, et al., Kremen proteins are Dickkopf receptors that regulate Wnt/beta-catenin signalling, Nature 417 (6889) (2002 Jun 6) 664–667. PubMed PMID: 12050670. Epub 2002/06/07. eng.
[19] B. Mao, C. Niehrs, Kremen2 modulates Dickkopf2 activity during Wnt/LRP6 signaling, Gene 302 (1–2) (2003 Jan 2) 179–183. PubMed PMID: 12527209. Epub 2003/01/16. eng.
[20] B.K. Brott, S.Y. Sokol, Regulation of Wnt/LRP signaling by distinct domains of Dickkopf proteins, Mol. Cell Biol. 22 (17) (2002 Sep) 6100–6110. PubMed PMID: 12167704. PMCID: PMC133995. Epub 2002/08/09. eng.
[21] C.Y. Fu, Y.F. Su, M.H. Lee, G.D. Chang, H.J. Tsai, Zebrafish Dkk3a protein regulates the activity of myf5 promoter through interaction with membrane receptor integrin α6b, J. Biol. Chem. 287 (47) (2012 Nov 16) 40031–40042. PubMed PMID: 23024366. PMCID: PMC3501020. Epub 2012/10/02. eng.
[22] R.J. Hsu, C.C. Lin, Y.F. Su, H.J. Tsai, dickkopf-3-related gene regulates the expression of zebrafish myf5 gene through phosphorylated p38a-dependent Smad4 activity, J. Biol. Chem. 286 (8) (2011 Feb 25) 6855–6864. PubMed PMID: 21159776. PMCID: PMC3057840. Epub 2010/12/17. eng.
[23] R.J. Hsu, C.Y. Lin, H.S. Hoi, S.K. Zheng, C.C. Lin, H.J. Tsai, Novel intronic microRNA represses zebrafish myf5 promoter activity through silencing dickkopf-3 gene, Nucleic Acids Res. 38 (13) (2010 Jul) 4384–4393. PubMed PMID: 20236986. PMCID: PMC2910042. Epub 2010/03/20. eng.
[24] J. Xu, X. Li, W. Chen, Z. Zhang, Y. Zhou, Y. Gou, et al., Myofiber Baf60c controls muscle regeneration by modulating Dkk3-mediated paracrine signaling, J. Exp. Med. 220 (9) (2023 Sep 4). PubMed PMID: 37284884. PMCID: PMC10250555. Epub 2023/06/07. eng.
[25] Q. Zhang, Y.X. Li, X.L. Li, Y. Yin, R.L. Li, X. Qiao, et al., A comparative study of the five-repetition sit-to-stand test and the 30-second sit-to-stand test to assess exercise tolerance in COPD patients, Int. J. Chronic Obstr. Pulm. Dis. 13 (2018) 2833–2839. PubMed PMID: 30237707. PMCID: PMC6136403. Epub 20180910. eng.
[26] J. Gao, M. Deng, Y. Li, Y. Yin, X. Zhou, Q. Zhang, et al., Resistin as a systemic inflammation-related biomarker for sarcopenia in patients with chronic obstructive pulmonary disease, Front. Nutr. 9 (2022) 921399. PubMed PMID: 35903456. PMCID: PMC9315354. Epub 20220712. eng.
[27] M. Deng, Y. Bian, Q. Zhang, X. Zhou, G. Hou, Growth differentiation factor-15 as a biomarker for sarcopenia in patients with chronic obstructive pulmonary disease, Front. Nutr. 9 (2022) 897097. PubMed PMID: 35845807. PMCID: PMC9282868. Epub 20220630. eng.
[28] M. Deng, Q. Zhang, L. Yan, Y. Bian, R. Li, J. Gao, et al., Glycyl-l-histidyl-l-lysine-Cu2+ rescues cigarette smoking-induced skeletal muscle dysfunction via a sirtuin 1-dependent pathway, Journal of Cachexia, Sarcopenia and Muscle 14 (3) (2023) 1365–1380.
[29] J.S. Zhou, Z.Y. Li, X.C. Xu, Y. Zhao, Y. Wang, H.P. Chen, et al., Cigarette smoke-initiated autoimmunity facilitates sensitisation to elastin-induced COPD-like pathologies in mice, Eur. Respir. J. 56 (3) (2020 Sep) 32366484. PubMed PMID, Epub 20200903. eng.
[30] J. Yin, L. Yang, Y. Xie, Y. Liu, S. Li, W. Yang, et al., Dkk3 dependent transcriptional regulation controls age related skeletal muscle atrophy, Nat. Commun. 9 (1) (2018 May 1) 1752. PubMed PMID: 29717119. PMCID: PMC5931527. Epub 20180501. eng.
[31] ATS statement: guidelines for the six-minute walk test, Am. J. Respir. Crit. Care Med. 166 (1) (2002 Jul 1) 111–117. PubMed PMID: 12091180. eng.
[32] T. Taivassalo, S.N. Hussain, Contribution of the mitochondria to locomotor muscle dysfunction in patients with COPD, Chest 149 (5) (2016 May) 1302–1312. PubMed PMID: 26836890. Epub 20151212. eng.
[33] X. Fang, J. Hu, Y. Chen, W. Shen, B. Ke, Dickkopf-3: current knowledge in kidney diseases, Front. Physiol. 11 (2020) 533344. PubMed PMID: 33391006. PMCID: PMC7772396. Epub 20201216. eng.
[34] T. Speer, S.J. Schunk, T. Sarakpi, D. Schmit, M. Wagner, L. Arnold, et al., Urinary DKK3 as a biomarker for short-term kidney function decline in children with chronic kidney disease: an observational cohort study, Lancet Child Adolesc Health 7 (6) (2023 Jun) 405–414. PubMed PMID: 37119829. Epub 20230426. eng.
[35] S.J. Schunk, A. Zarbock, M. Meersch, M. Küllmar, J.A. Kellum, D. Schmit, et al., Association between urinary dickkopf-3, acute kidney injury, and subsequent loss of kidney function in patients undergoing cardiac surgery: an observational cohort study, Lancet 394 (10197) (2019 Aug 10) 488–496. PubMed PMID: 31202596. Epub 20190612. eng.
[36] G. Roscigno, C. Quintavalle, G. Biondi-Zoccai, F. De Micco, G. Frati, A. Affinito, et al., Urinary dickkopf-3 and contrast-associated kidney damage, J. Am. Coll. Cardiol. 77 (21) (2021 Jun 1) 2667–2676. PubMed PMID: 34045024. eng.
[37] S.J. Schunk, C. Beisswenger, F. Ritzmann, C. Herr, M. Wagner, S. Triem, et al., Measurement of urinary Dickkopf-3 uncovered silent progressive kidney injury in patients with chronic obstructive pulmonary disease, Kidney Int. 100 (5) (2021 Nov) 1081–1091. PubMed PMID: 34237325. Epub 20210706. eng.
[38] R. Qaisar, A. Karim, T. Muhammad, I. Shah, Circulating biomarkers of accelerated sarcopenia in respiratory diseases, Biology 9 (10) (2020 Oct 3). PubMed PMID: 33023021. PMCID: PMC7600620. Epub 20201003. eng.
[39] Z. Gan, T. Fu, D.P. Kelly, R.B. Vega, Skeletal muscle mitochondrial remodeling in exercise and diseases, Cell Res. 28 (10) (2018 Oct) 969–980. PubMed PMID: 30108290. PMCID: PMC6170448. Epub 20180814. eng.
[40] C.E. Fealy, L. Grevendonk, J. Hoeks, M.K.C. Hesselink, Skeletal muscle mitochondrial network dynamics in metabolic disorders and aging, Trends Mol. Med. 27 (11) (2021 Nov) 1033–1044. PubMed PMID: 34417125. Epub 20210817. eng.
[41] Y. Wang, P. Li, Y. Cao, C. Liu, J. Wang, W. Wu, Skeletal muscle mitochondrial dysfunction in chronic obstructive pulmonary disease: underlying mechanisms and physical therapy perspectives, Aging Dis 14 (1) (2023 Feb 1) 33–45. PubMed PMID: 36818563. PMCID: PMC9937710. Epub 20230201. eng.
[42] A. Ito, M. Hashimoto, J. Tanihata, S. Matsubayashi, R. Sasaki, S. Fujimoto, et al., Involvement of Parkin-mediated mitophagy in the pathogenesis of chronic obstructive pulmonary disease-related sarcopenia, J Cachexia Sarcopenia Muscle 13 (3) (2022 Jun) 1864–1882. PubMed PMID: 35373498. PMCID: PMC9178376. Epub 20220403. eng.
[43] A. Kikuchi, K. Fumoto, H. Kimura, The Dickkopf1-cytoskeleton-associated protein 4 axis creates a novel signalling pathway and may represent a molecular target for cancer therapy, Br. J. Pharmacol. 174 (24) (2017 Dec) 4651–4665. PubMed PMID: 28514532. PMCID: PMC5727324. Epub 20170707. eng.
[44] G.P. Suchitha, R.D.A. Balaya, R. Raju, T.S. Keshava Prasad, S. Dagamajalu, A network map of cytoskeleton-associated protein 4 (CKAP4) mediated signaling pathway in cancer, J Cell Commun Signal 17 (3) (2023 Sep) 1097–1104. PubMed PMID: 36944905. PMCID: PMC10409693. Epub 20230321. eng.
[45] H. Kimura, H. Yamamoto, T. Harada, K. Fumoto, Y. Osugi, R. Sada, et al., CKAP4, a DKK1 receptor, is a biomarker in exosomes derived from pancreatic cancer and a molecular target for therapy, Clin. Cancer Res. 25 (6) (2019 Mar 15) 1936–1947. PubMed PMID: 30610103. Epub 20190104. eng.
[46] J.M. Siegfried, Women and lung cancer: does oestrogen play a role? Lancet Oncol. 2 (8) (2001) 506–513.
[47] L. Erfinanda, K. Ravindran, F. Kohse, K. Gallo, R. Preissner, T. Walther, et al., Oestrogen-mediated upregulation of the Mas receptor contributes to sex differences in acute lung injury and lung vascular barrier regulation, Eur. Respir. J. 57 (1) (2021 Jan). PubMed PMID: 32764118. Epub 20210121. eng.
[48] A. Tam, A. Churg, J.L. Wright, S. Zhou, M. Kirby, H.O. Coxson, et al., Sex differences in airway remodeling in a mouse model of chronic obstructive pulmonary disease, Am. J. Respir. Crit. Care Med. 193 (8) (2016 Apr 15) 825–834. PubMed PMID: 26599602. eng.
[49] A. Pellegrino, P.M. Tiidus, R. Vandenboom, Mechanisms of estrogen influence on skeletal muscle: mass, regeneration, and mitochondrial function, Sports Med. 52 (12) (2022 Dec) 2853–2869. PubMed PMID: 35907119. Epub 20220730. eng.
[50] Global Initiative for Chronic Obstructive Lung Disease. Global Strategy For Prevention, Diagnosis and Management Of COPD: 2023 Report. Available from: http://www.goldcopd.org.
[51] L.F. Fitzgerald, J. Lackey, A. Moussa, S.V. Shah, A.M. Castellanos, S. Khan, et al., Chronic aryl hydrocarbon receptor activity impairs muscle mitochondrial function with tobacco smoking, J Cachexia Sarcopenia Muscle 15 (2) (2024 Apr) 646–659. PubMed PMID: 38333944. PMCID: PMC10995249. Epub 20240209. eng.
[52] T. Thome, K. Miguez, A.J. Willms, S.K. Burke, V. Chandran, A.R. de Souza, et al., Chronic aryl hydrocarbon receptor activity phenocopies smoking-induced skeletal muscle impairment, J Cachexia Sarcopenia Muscle 13 (1) (2022 Feb) 589–604. PubMed PMID: 34725955. PMCID: PMC8818603. Epub 20211101. eng.
[53] G.Z. Wang, L. Zhang, X.C. Zhao, S.H. Gao, L.W. Qu, H. Yu, et al., The Aryl hydrocarbon receptor mediates tobacco-induced PD-L1 expression and is associated with response to immunotherapy, Nat. Commun. 10 (1) (2019 Mar 8) 1125. PubMed PMID: 30850589. PMCID: PMC6408580. Epub 20190308. eng.